Supplementary Information

Supplementary text for Figure S1

The 3D-PSSM and 3D-JIGSAW comparative modeling servers were used to investigate whether E4-ORF1 is structurally related to any proteins in the structure database (Bates *et al.*, 2001; Kelley *et al.*, 2000). In agreement with results showing that *E4-ORF1* evolved from a *dUTPase* gene, both searches predicted with >99.7% confidence that E4-ORF1 adopts a protein fold like that of five structurally-related trimeric dUTPase enzymes (*H. sapiens*, *E. coli*, *M. tuberculosis*, feline immunodeficiency virus, equine infectious anemia virus). No other matches were found. Among the five enzymes, human dUTPase shares the highest sequence similarity with E4-ORF1 (Weiss *et al.*, 1997), so we also used 3D-JIGSAW to model E4-ORF1 to the crystal structure of this enzyme. This analysis predicted that the secondary structure organization and protein fold of E4-ORF1 are strikingly similar to those of the monomeric subunit in a human dUTPase trimer (**Figure S1**).

Titles and legends to Figures

Figure S1. E4-ORF1 has a predicted protein fold similar to trimeric dUTPases. E4-ORF1 has a similar predicted (**a**) secondary structure organization and (**b**) protein fold as human dUTPase. In (a), E4-ORF1 and dUTPase sequences are aligned. Arrows or wavy lines depict β-strands or α-helices, respectively. Four residues defining the E4-ORF1 PBM element are underlined. In (b), ribbon diagrams of E4-ORF1 (*top*) modeled to the crystal structure of the monomeric subunit in a dUTPase trimer (*bottom*) are shown. In the diagrams, the first two E4-ORF1 residues and last five dUTPase residues are not visible, and the E4-ORF1 PBM and

dUTPase P-loop motif are red highlighted. Structural illustrations were created with MacPyMol software (DeLano Scientific LLC).

Figure S2. Purified E4-ORF1 forms a homo-trimer. (**a**) Protein gel analysis verifies purification of FLAG-HA-E4-ORF1 to homogeneity. 293T cells were transfected with pGW1 coding for FLAG-HA-E4-ORF1, and cell extracts were prepared in RIPA buffer. FLAG-HA-E4-ORF1 was immunoprecipitated with FLAG M2 monoclonal antibody (Sigma-Aldrich) from 1 mg of cell extract. Beads were washed with RIPA buffer, equilibrated with elution buffer (50 mM Tris-HCl, pH8.0, 0.15 M NaCl, 0.1% DOC), and incubated with 30 μL of elution buffer containing 0.2 mg/mL FLAG peptide (Sigma-Aldrich Co.) for 3h at RT. Half of the eluted FLAG-HA-E4-ORF1 protein was resolved by SDS-PAGE and visualized with Silver Stain Plus (Bio-Rad Laboratories). (**b**) Purified FLAG-HA-E4-ORF1 forms homo-trimers. The remaining half of FLAG-HA-E4-ORF1 purified above in (A) was fractionated by SEC with elution buffer containing 0.1% DOC, which quantitatively converts E4-ORF1 to its trimeric form (see Figure 1b). Fractions were immunoblotted with FLAG antibody. Purified 16-kD double epitope-tagged FLAG-HA-E4-ORF1 elutes at 47-kD, nearly identical to the predicted 48-kD mass of a trimer.

Figure S3. Carboxyl-terminal dUTPase residues overlapping β8 determine trimer formation. These data show that *wt* dUTPase and ΔC16 with β8 intact elute as a trimer by SEC and self-associate in pulldown assays whereas ΔC20 with β8 partially truncated elutes as a monomer and fails to self-associate. (**a**) A deletion in β8 abolishes dUTPase trimer formation. 293T cells were transfected with pGW1 coding for the indicated His-dUTPase protein. Cell extracts in RIPA buffer were fractionated by SEC with elution buffer containing 0.1% DOC.

Fractions were immunoblotted with His antibody. (**b**) A deletion in β8 also abolishes self-association of dUTPase. 293T cells were co-transfected with an equal amount of pGW1 coding for the indicated His- and HA-dUTPase protein. Cell extracts prepared in NETN buffer were incubated with Ni-NTA beads (QIAGEN, Inc) for 3h at 4°C to recover His-dUTPase. Beads were extensively washed with NETN buffer and boiled in sample buffer to elute bound proteins. Such proteins (*left*) and total cell extracts (Input) (*right*) were immunoblotted with HA or His antibody.

Figure S4. E4-ORF1 β8 residues determine trimer formation. (**a**) β8 deletion abolishes E4-ORF1 trimer formation. 293T cells were transfected with pGW1 encoding ΔC5 or ΔC7. Extracts in RIPA buffer were fractionated by SEC with elution buffer containing 0.1% DOC (see Figure 1b legend). (**b**) β8 deletion or mutation abolishes E4-ORF1 self-association. 293T cells were co-transfected with two pGW1 plasmids encoding the same HA-tagged and untagged E4-ORF1 protein. Extracts in RIPA buffer were IP'd with HA antibody. Recovered proteins and total cell extracts (Input) were blotted with E4-ORF1 antibody.

Note: We were unable to test the predicted requirement for E4-ORF1 β1 in trimer formation because deletion or substitution mutations in this element invariably resulted in aberrantly aggregated proteins; however, the finding that monomeric ΔC7 co-IP'd with *wt* E4-ORF1 (unpublished data) supports the idea that β1-β8 interactions mediate trimer formation.

Figure S5. E4-ORF1 binds cooperatively to PDZ domains in Dlg1 but not MAGI-1. (**a**) Disruption of either Dlg1 PDZ1 or PDZ2 abrogates binding to E4-ORF1. 293 cells were transfected with pGW1 (-) or pGW1 encoding *wt* E4-ORF1 or negative control PBM mutant IIIA (see Figure 2a) in combination with pEGFP encoding GFP-tagged *wt* Dlg1 (pEGFP-C3 encoding

GFP-Dlg1-I3) (Frese *et al.*, 2006) or PDZ1* (1*), PDZ2* (2*), or PDZ1*+2* (1*+2*). Extracts in RIPA buffer were IP'd with E4-ORF1 antibody. Recovered proteins and total cell extracts (Input) were blotted with E4-ORF1 or Dlg1 antibody. GLG residues in the conserved GLGF motifs of PDZ1 and/or PDZ2 were replaced with alanine residues to create Dlg1 PDZ1*, PDZ2*, and PDZ1*+2*. The data are consistent with the report that E4-ORF1 binds to isolated Dlg1 PDZ1+2 but not PDZ1 or PDZ2 in GST pulldown assays (Frese *et al.*, 2006). PDZ tandems comprise a single conformational unit that functions either to stabilize PDZ domain structure (Feng *et al.*, 2003) or to mediate cooperative interactions with multimeric ligands (Grembecka *et al.*, 2006; Grootjans *et al.*, 2000; Long *et al.*, 2003). Data presented here suggest that the Dlg1 PDZ tandem serves the latter function for an E4-ORF1 trimer, which is the first reported protein to bind cooperatively to this functional unit. Notably, the HPV E6 and HTLV-1 Tax oncoproteins and the cellular APC tumor suppressor protein also have a carboxyl-terminal PBM that mediates binding to Dlg1 via the PDZ tandem, and these interactions mediate either viral oncoprotein-induced cellular transformation (Hirata *et al.*, 2004; Kiyono *et al.*, 1997) or APC-dependent directed cell migration (Etienne-Manneville *et al.*, 2005). As HPV E6 forms a large oligomer (Garcia-Alai *et al.*, 2007) and HTLV-1 Tax and APC form homo-dimers (Day & Alber, 2000; Tie *et al.*, 1996), these proteins may also bind cooperatively to the Dlg1 PDZ tandem. (**b**) Deletion of MAGI-1 PDZ1 or PDZ3 alone fails to abrogate binding to E4-ORF1. 293 cells were transfected with pGW1 (-) or pGW1 encoding *wt* E4-ORF1 or PBM mutant IIIA in combination with pGW1 encoding HA-tagged *wt* MAGI-1 or PDZΔ1 (Δ1), PDZΔ3 (Δ3), or PDZΔ1Δ3 (Δ1Δ3). Extracts in RIPA buffer were IP'd with HA antibody. Recovered proteins and total cell extracts (Input) were blotted with E4-ORF1 or HA antibody. The amount of *wt* MAGI-1 co-precipitated with *wt* E4-ORF1 was quantified by densitometry and assigned an arbitrary value

of 1. Intensity values for co-precipitated MAGI-1 mutants are relative to this standard. Densitometric measurements were made using the Personal Densitometer SI apparatus and ImageQuant software (Molecular Dynamics).

Figure S6. Monomeric E4-ORF1 mutant AAA binds MUPP1. 293 cells were transfected with pGW1 coding for HA-MUPP1 in combination with empty pGW1 (vector) or pGW1 coding for *wt* E4-ORF1 (*wt*) or the indicated mutant E4-ORF1. PBM mutant IIIA (see Figure 2a) was included as a negative control. Cell extracts prepared in RIPA buffer were immunoprecipitated with HA antibody. Recovered proteins and total cell extracts (Input) were immunoblotted with HA or E4-ORF1 antibody.

Figure S7. E4-ORF1 trimers fail to bind MUPP1, MAGI-1, and ZO-2. (**a-c**). E4-ORF1 trimers fail to bind (a) MUPP1 PDZ10, (b) MAGI-1 PDZ1, and (c) ZO-2 PDZ1. Experiments identical to those shown in Figures 3c-e were conducted, except that the SEC elution buffer contained 0.1% DOC to convert E4-ORF1 to its trimeric form. When expressed alone, E4-ORF1 eluted as a 39-kD trimer, whereas MUPP1 PDZ10 and ZO-2 PDZ1 eluted as 26-kD dimers and MAGI-1 PDZ1 eluted as a 13-kD monomer. These data suggest that DOC displaces E4-ORF1 monomers bound to the PDZ domains by inducing such monomers to form free trimers, although this effect was more pronounced in SEC analyses than in co-IP assays where complexes of E4-ORF1 associated with full-length MUPP1, MAGI-1, or ZO-2 could be detected in cell extracts prepared with DOC-containing RIPA buffer.

Figure S8. E4-ORF1 TRI element mutants have defects in binding to endogenous Dlg1 in CREF cells. CREF cells were transduced with empty pBABE retrovirus (vector) or pBABE retrovirus coding for *wt* E4-ORF1 (*wt*) or the indicated mutant E4-ORF1. Cell extracts in RIPA

buffer were immunoprecipitated with E4-ORF1 antibody. Recovered proteins and total cell extracts (Input) were immunoblotted with Dlg1 or E4-ORF1 antibody.

Figure S9. E4-ORF1 TRI element mutants have defects in PKB activation and cellular transformation. (**a**) E4-ORF1 TRI element mutants have defects in activating PKB. 3T3 cells were transfected with pGW1 (vector) or pGW1 encoding *wt* or the indicated mutant E4-ORF1. Extracts of cells (serum starved for 16h) were blotted with phospho-PKB (Thr308) or PKB (Cell Signaling Technology), or E4-ORF1 antibody. Vertical lines between samples indicate removal of irrelevant lanes. (**b**) E4-ORF1 TRI element mutants have defects in focus formation. CREF cells were transfected with pJ4Ω (vector) or pJ4Ω encoding *wt* or the indicated mutant E4-ORF1. At three-weeks post-transfection, the number of transformed foci induced by *wt* E4-ORF1 was assigned an arbitrary value of 100%, and the focus-forming activity for each mutant is relative to this standard. Shown are the mean and standard deviation of data compiled from two independent experiments performed in duplicate. Focus formation assays were carried out as described (Weiss *et al.*, 1997).

Figure S10. E4-ORF1 mutant AAA+KI but not VAA+KI fails to form trimers. 293T cells were transfected with pGW1 coding for VAA+KI or pBABE coding for AAA+KI. Cell extracts in RIPA buffer were fractionated by SEC with elution buffer containing 0.1% DOC and blotted with E4-ORF1 antibody.

Figure S11. Fusion to dimeric GST restores Dlg1 binding to mutant AAA+KI in a GST pulldown assay. The indicated E4-ORF1 protein fused to GST was incubated with extracts of CREF cells prepared in RIPA buffer. Bound proteins were immunoblotted with Dlg1 antibody (*upper panel*). Coomassie staining verified the use of an equal amount of each GST

fusion protein (*lower panel*). Vertical lines between the *wt* and AAA+KI samples indicate removal of irrelevant lanes.

Figure S12. Monomeric AAA+KI fails to promote Dlg1 translocation to the plasma membrane. (**a**) 293T cells were co-transfected with pEGFP encoding Dlg1 and pBABE (vector) or pBABE encoding *wt* or the indicated mutant E4-ORF1. 293T cells on coverslips coated with 0.001% poly-L-lysine (Sigma Diagnostics) were fixed with 4% paraformaldehyde (Polysciences) for 20 min at RT. Coverslips were mounted onto slides with Slowfade Light (Molecular Probes). Cells were visualized and photographed with a Zeiss Axioplan 2 epifluorescent microscope attached to a CoolSnap HQ CCD camera (Photometrics). (**b**) Quantification of E4-ORF1-induced Dlg1 membrane translocation. Values (average and range) for each sample represent percentages of GFP-positive cells showing GFP-Dlg1 accumulation at the plasma membrane. Data were combined from two independent experiments examining greater than 120 GFP-positive cells per sample.

The capacity of E4-ORF1 to promote either sequestration (**Figure 3b**) or membrane translocation of a PDZ protein target (**this Supplementary Figure**) correlates with a monomer or trimer, respectively, suggesting that an undiscovered element specifically active in a monomer or trimer determines these divergent consequences. The PDZ protein target likely also contributes to the outcome, however, given that membrane translocation of Dlg1 depends on not only E4-ORF1 but also several different Dlg1 domains, including PDZ1+2, I3, and either SH3 or US3 (Frese *et al*., 2006).

Figure S13. An E4-ORF1 dimer binds to the Dlg1 PDZ1+2 tandem in the absence of DOC. Identical SEC analyses to those described in Figure 5c were conducted, except that the elution buffer lacked DOC in an attempt to convert E4-ORF1 to monomers. When expressed alone,

wt E4-ORF1 and Dlg1 PDZ1+2 eluted as 12-kD or 23-kD monomers, respectively, but when co-expressed, both proteins co-eluted at 46-kD, similar to the predicted 50-kD mass for a heterocomplex composed of two E4-ORF1 molecules bound to one Dlg1 PDZ1+2 molecule. Given compelling evidence indicating that only oligomeric E4-ORF1 could form such a heterocomplex (see Figure 5b and Supplementary Figures S5a & S12), these two E4-ORF1 molecules must represent a dimer rather than separate monomers. In this regard, only two of three subunits in an E4-ORF1 trimer can interact with the Dlg1 PDZ tandem, suggesting that the lack of DOC causes the single unbound E4-ORF1 subunit to dissociate and that the resulting E4-ORF1 dimer is stabilized by its TRI element-dependent cooperative interaction with the Dlg1 PDZ tandem. Based on this reasoning and our cumulative results, we conclude that an E4-ORF1 dimer but not monomers stably interact with the Dlg1 PDZ tandem under the conditions of this experiment.

References

Bates PA, Kelley LA, MacCallum RM and Sternberg MJ. (2001). Enhancement of protein modeling by human intervention in applying the automatic programs 3D-JIGSAW and 3D-PSSM. *Proteins* **45**: 39-46.

Day CL and Alber T. (2000). Crystal structure of the amino-terminal coiled-coil domain of the APC tumor suppressor. *J Mol Biol* **301**: 147-156.

Etienne-Manneville S, Manneville JB, Nicholls S, Ferenczi MA and Hall A. (2005). Cdc42 and Par6-PKCzeta regulate the spatially localized association of Dlg1 and APC to control cell polarization. *J Cell Biol* **170**: 895-901.

Feng W, Shi Y, Li M and Zhang M. (2003). Tandem PDZ repeats in glutamate receptor-interacting proteins have a novel mode of PDZ domain-mediated target binding. *Nat Struct Biol* **10**: 972-978.

Frese KK, Latorre IJ, Chung SH, Caruana G, Bernstein A, Jones SN, *et al.* (2006). Oncogenic function for the Dlg1 mammalian homolog of the Drosophila discs-large tumor suppressor. *EMBO J* **25**: 1406-1417.

Garcia-Alai MM, Dantur KI, Smal C, Pietrasanta L and de Prat-Gay G. (2007). High-risk HPV E6 oncoproteins assemble into large oligomers that allow localization of endogenous species in prototypic HPV-transformed cell lines. *Biochemistry* **46**: 341-349.

Grembecka J, Cierpicki T, Devedjiev Y, Derewenda U, Kang BS, Bushweller JH, *et al.* (2006). The binding of the PDZ tandem of syntenin to target proteins. *Biochemistry* **45**: 3674-3683.

Grootjans JJ, Reekmans G, Ceulemans H and David G. (2000). Syntenin-syndecan binding requires syndecan-synteny and the co-operation of both PDZ domains of syntenin. *J Biol Chem* **275**: 19933-19941.

Hirata A, Higuchi M, Niinuma A, Ohashi M, Fukushi M, Oie M, *et al.* (2004). PDZ domain-binding motif of human T-cell leukemia virus type 1 Tax oncoprotein augments the transforming activity in a rat fibroblast cell line. *Virology* **318**: 327-336.

Kelley LA, MacCallum RM and Sternberg MJ. (2000). Enhanced genome annotation using structural profiles in the program 3D-PSSM. *J Mol Biol* **299**: 499-520.

Kiyono T, Hiraiwa A, Fujita M, Hayashi Y, Akiyama T and Ishibashi M. (1997). Binding of high-risk human papillomavirus E6 oncoproteins to the human homologue of the Drosophila discs large tumor suppressor protein. *Proc Natl Acad Sci USA* **94**: 11612-11616.

Long JF, Tochio H, Wang P, Fan JS, Sala C, Niethammer M, *et al*. (2003). Supramodular structure and synergistic target binding of the N-terminal tandem PDZ domains of PSD-95. *J Mol Biol* **327**: 203-214.

Tie F, Adya N, Greene WC and Giam CZ. (1996). Interaction of the human T-lymphotropic virus type 1 Tax dimer with CREB and the viral 21-base-pair repeat. *J Virol* **70**: 8368-8374.

Weiss RS, Lee SS, Prasad BV and Javier RT. (1997). Human adenovirus early region 4 open reading frame 1 genes encode growth-transforming proteins that may be distantly related to dUTP pyrophosphatase enzymes. *J Virol* **71**: 1857-1870.

Fig. S1

a.

```
E4-ORF1   MAESLYAFIDSPGGIAPVQEGT-SNRYTFFCPESFHIP  37
dUTPase   --MQLRFARLSEHATAPTRGSARAAGYDLYSAYDYTIP  36
            β1                    β2     β2b

E4-ORF1   PHGVVLLHLKVSVLVPTGYQGRFMALNDYHARDILT-Q  74
dUTPase   PMEKAVVKTDIQIALPSGCYGRVAPRSGLAAKHFIDVG  74
            β3a   β3b    β4      α1     β5a

E4-ORF1   SDVIFAGRRQELTVLLFNHTDRFLYVRKGHPVGTLLLE  112
dUTPase   AGVIDEDYRGNVGVVLFNFGKEKFEVKKGDRIAQLICE  112
            β5b     β6      β6b     β7

E4-ORF1   RVIFPSVKIATLV----------------  125
dUTPase   RIFYPEIEEVQALDDTERGSGGFGSTGKN  141
            β8
```

b.

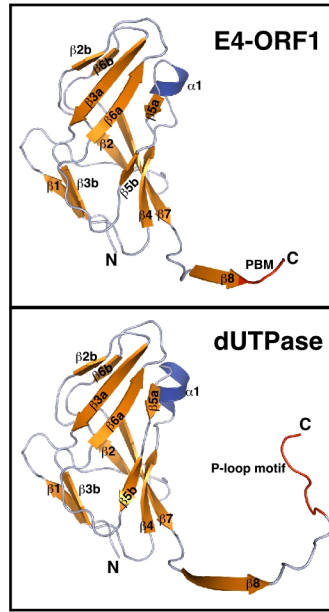

Fig. S2

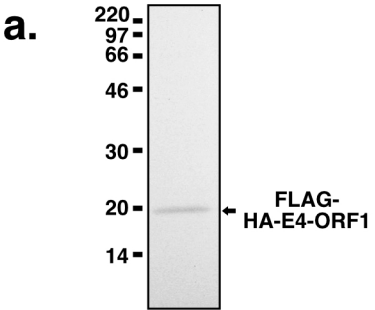
a.
220
97
66
46
30
20
14
FLAG-
HA-E4-ORF1

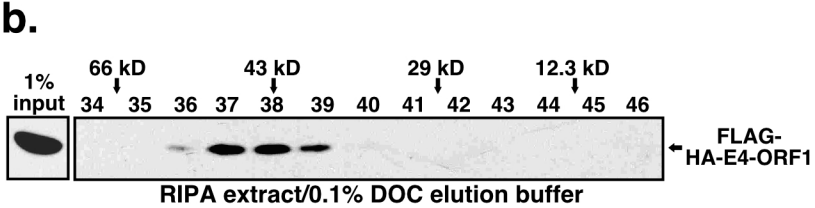
b.
1%
input
66 kD
43 kD
29 kD
12.3 kD
34
35
36
37
38
39
40
41
42
43
44
45
46
FLAG-
HA-E4-ORF1
RIPA extract/0.1% DOC elution buffer

Fig. S3

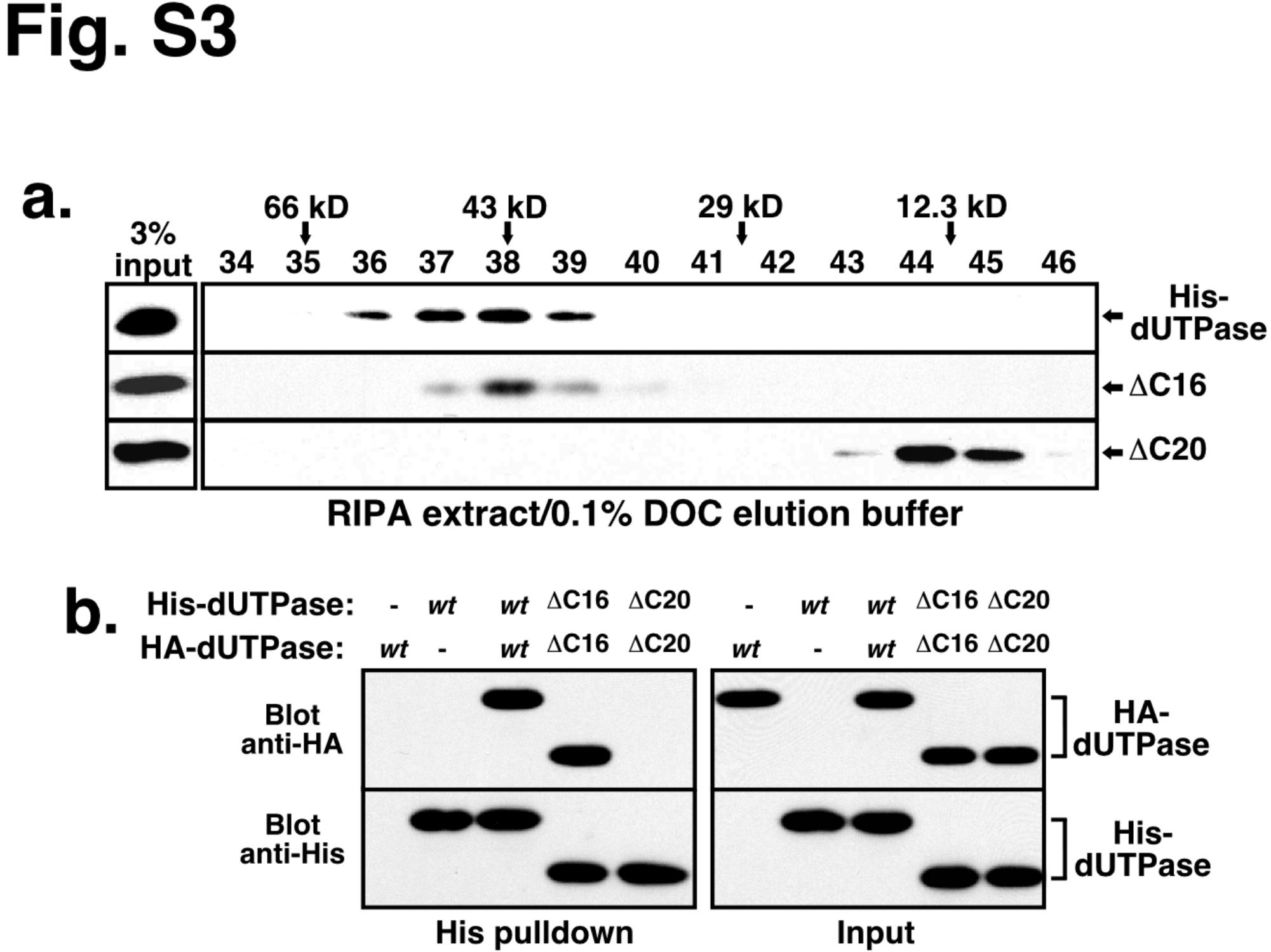
a.
66 kD
43 kD
29 kD
12.3 kD
3% input
34 35 36 37 38 39 40 41 42 43 44 45 46
His-dUTPase
ΔC16
ΔC20
RIPA extract/0.1% DOC elution buffer
b.
His-dUTPase: - wt wt ΔC16 ΔC20 - wt wt ΔC16 ΔC20
HA-dUTPase: wt - wt ΔC16 ΔC20 wt - wt ΔC16 ΔC20
Blot anti-HA
Blot anti-His
HA-dUTPase
His-dUTPase
His pulldown
Input

Fig. S4

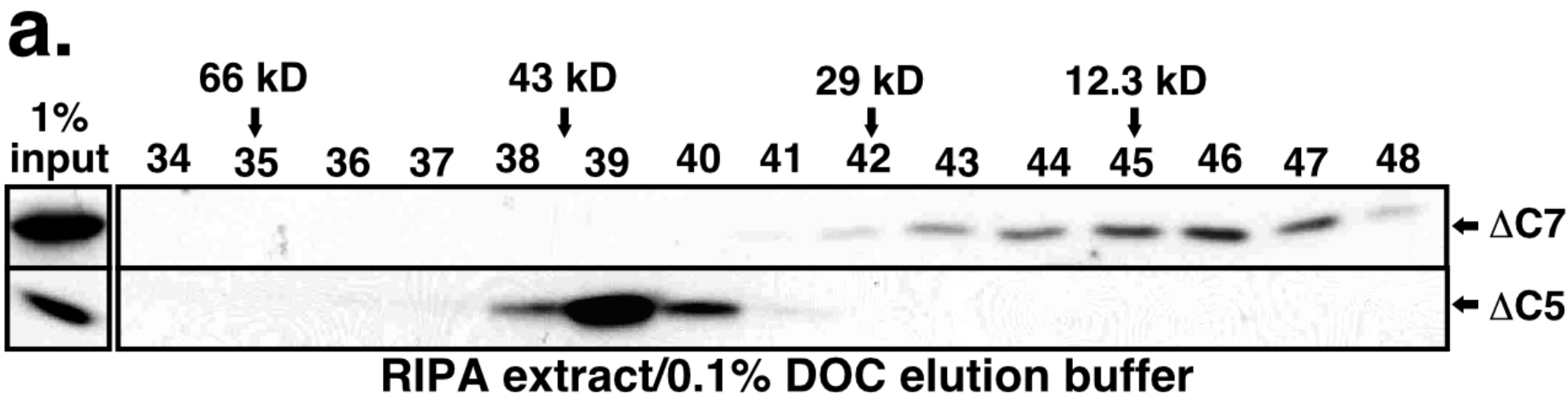
a.
66 kD
43 kD
29 kD
12.3 kD
1% input
34
35
36
37
38
39
40
41
42
43
44
45
46
47
48
ΔC7
ΔC5
RIPA extract/0.1% DOC elution buffer

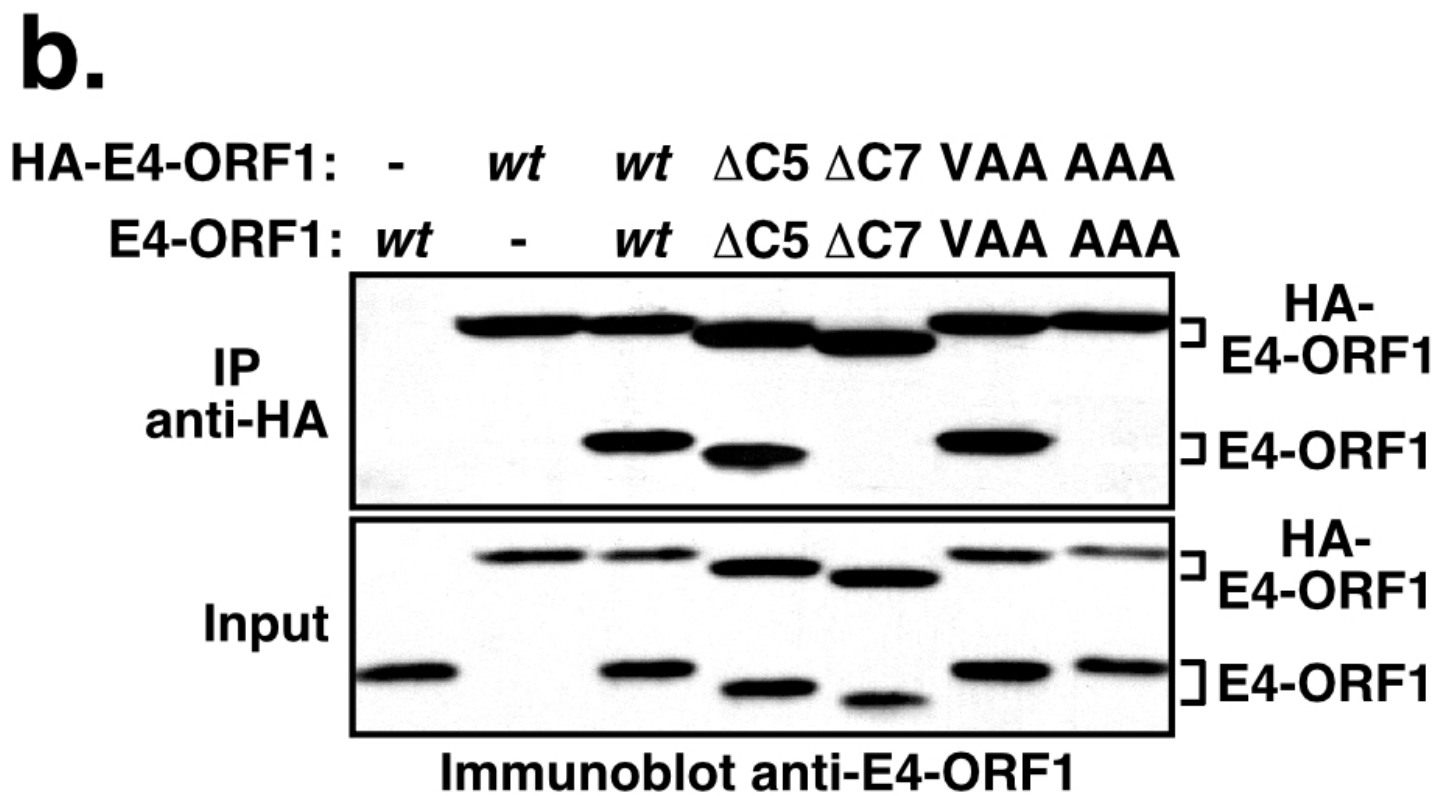
b.
HA-E4-ORF1: - wt wt ΔC5 ΔC7 VAA AAA
E4-ORF1: wt - wt ΔC5 ΔC7 VAA AAA
IP anti-HA
HA-E4-ORF1
E4-ORF1
Input
HA-E4-ORF1
E4-ORF1
Immunoblot anti-E4-ORF1

Fig. S5

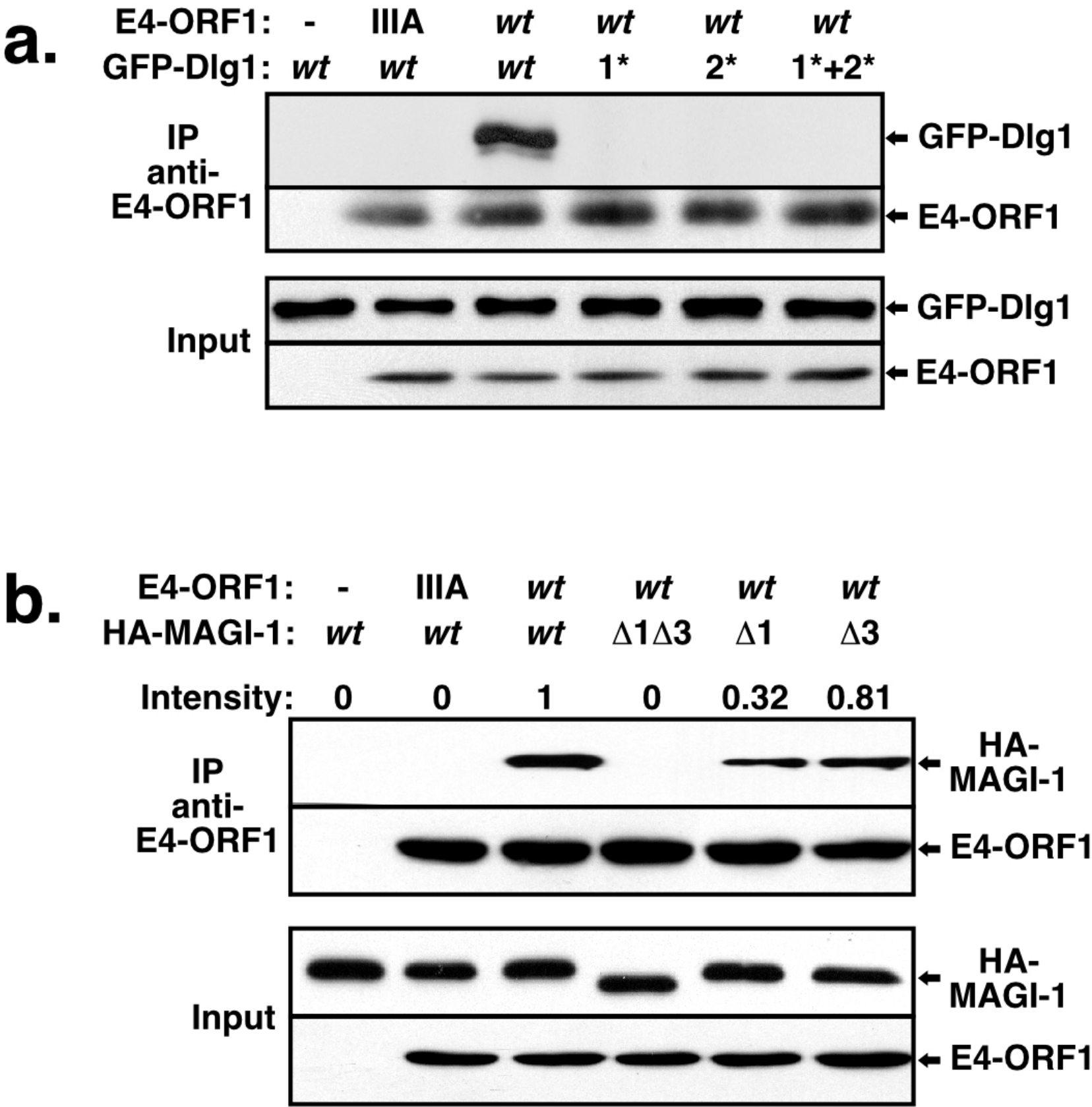
a.
E4-ORF1: - IIIA wt wt wt wt
GFP-Dlg1: wt wt wt 1* 2* 1*+2*
IP anti-E4-ORF1
GFP-Dlg1
E4-ORF1
Input
GFP-Dlg1
E4-ORF1
b.
E4-ORF1: - IIIA wt wt wt wt
HA-MAGI-1: wt wt wt Δ1Δ3 Δ1 Δ3
Intensity: 0 0 1 0 0.32 0.81
IP anti-E4-ORF1
HA-MAGI-1
E4-ORF1
Input
HA-MAGI-1
E4-ORF1

Fig. S6

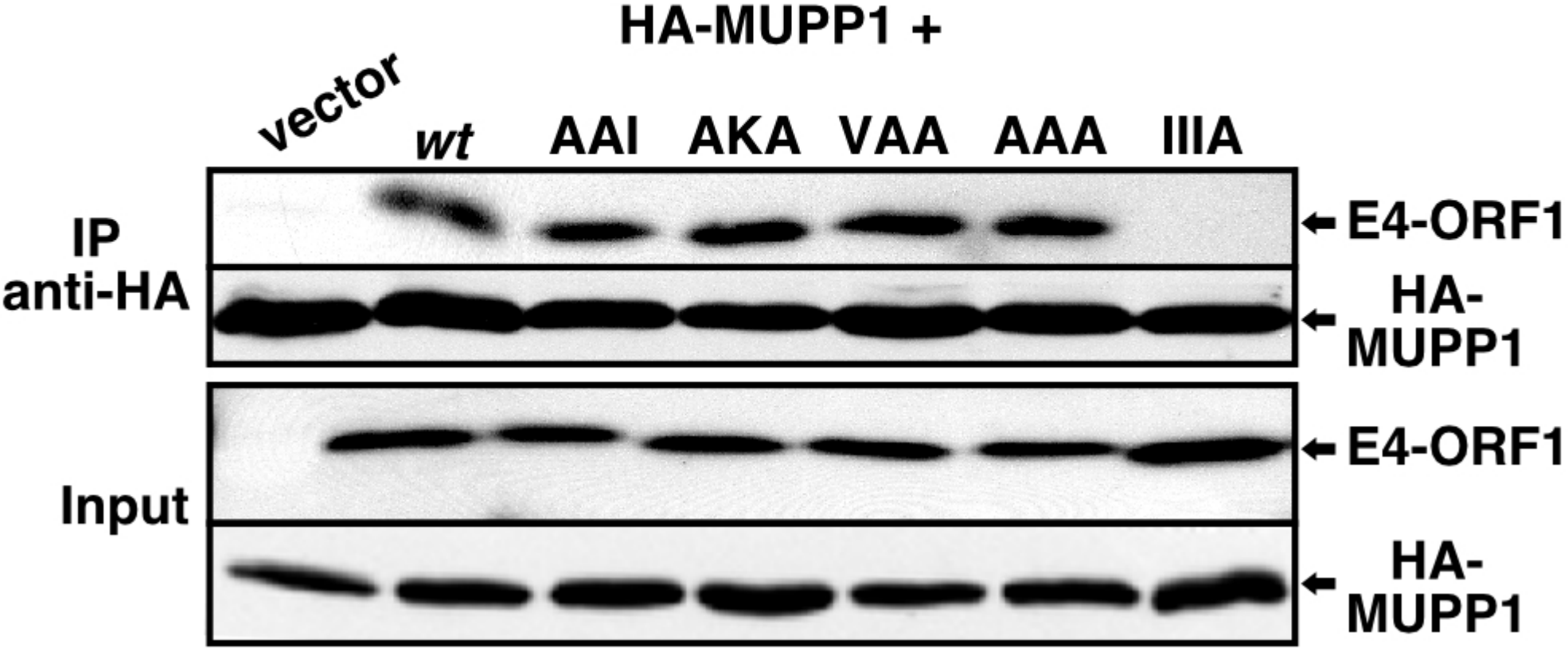
HA-MUPP1 +
vector
wt
AAI
AKA
VAA
AAA
IIIA
IP
anti-HA
E4-ORF1
HA-
MUPP1
Input
E4-ORF1
HA-
MUPP1

Fig. S7

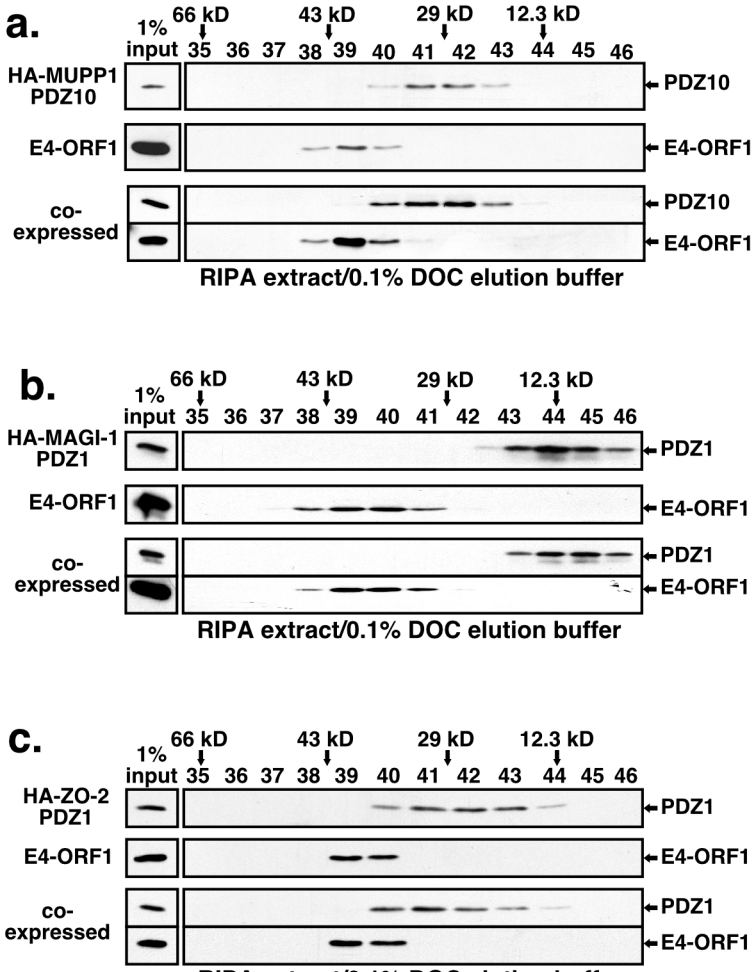
a.
1% input
66 kD
43 kD
29 kD
12.3 kD
35 36 37 38 39 40 41 42 43 44 45 46
HA-MUPP1 PDZ10
E4-ORF1
co-expressed
PDZ10
E4-ORF1
PDZ10
E4-ORF1
RIPA extract/0.1% DOC elution buffer
b.
1% input
66 kD
43 kD
29 kD
12.3 kD
35 36 37 38 39 40 41 42 43 44 45 46
HA-MAGI-1 PDZ1
E4-ORF1
co-expressed
PDZ1
E4-ORF1
PDZ1
E4-ORF1
RIPA extract/0.1% DOC elution buffer
c.
1% input
66 kD
43 kD
29 kD
12.3 kD
35 36 37 38 39 40 41 42 43 44 45 46
HA-ZO-2 PDZ1
E4-ORF1
co-expressed
PDZ1
E4-ORF1
PDZ1
E4-ORF1
RIPA extract/0.1% DOC elution buffer

Fig. S8

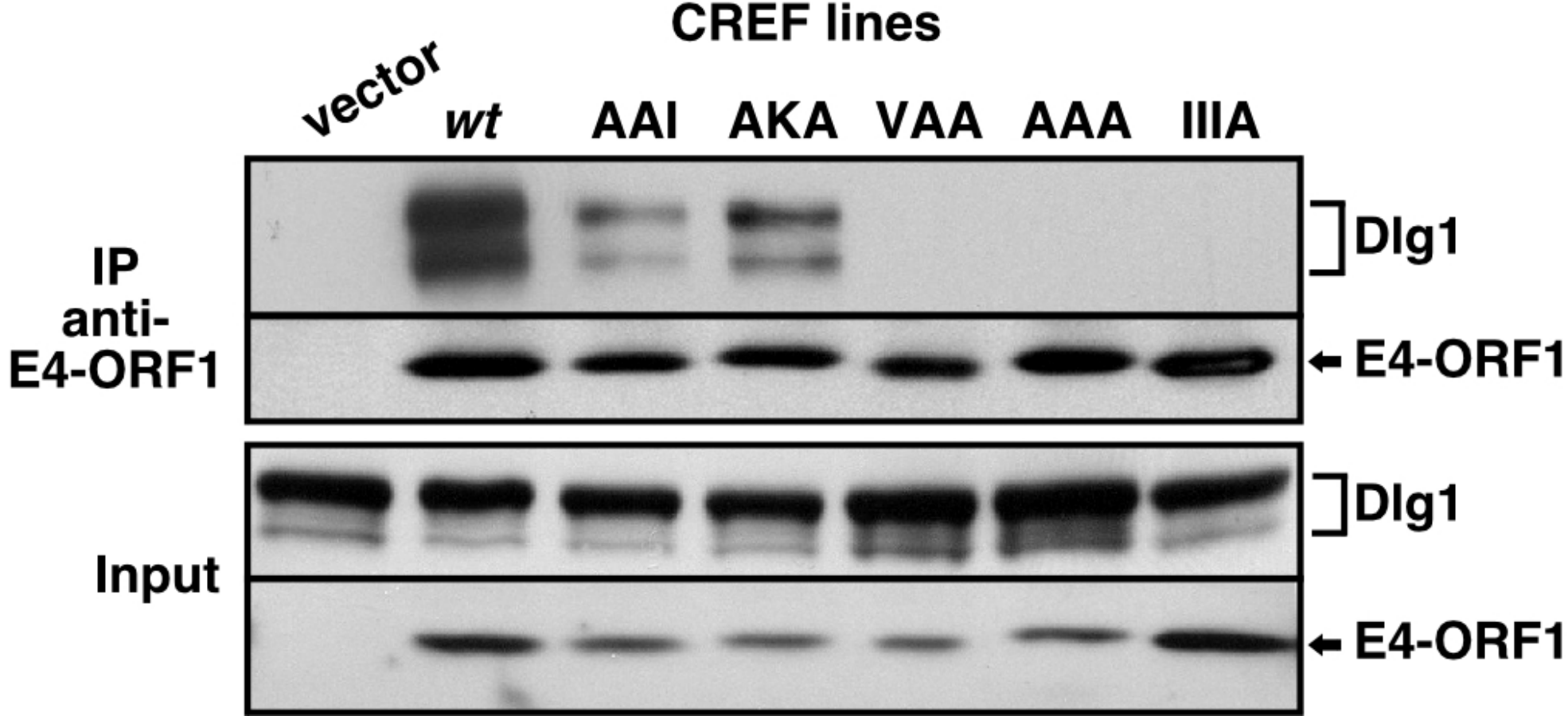
CREF lines
vector
wt
AAI
AKA
VAA
AAA
IIIA
IP
anti-
E4-ORF1
Dlg1
E4-ORF1
Input
Dlg1
E4-ORF1

Fig. S9

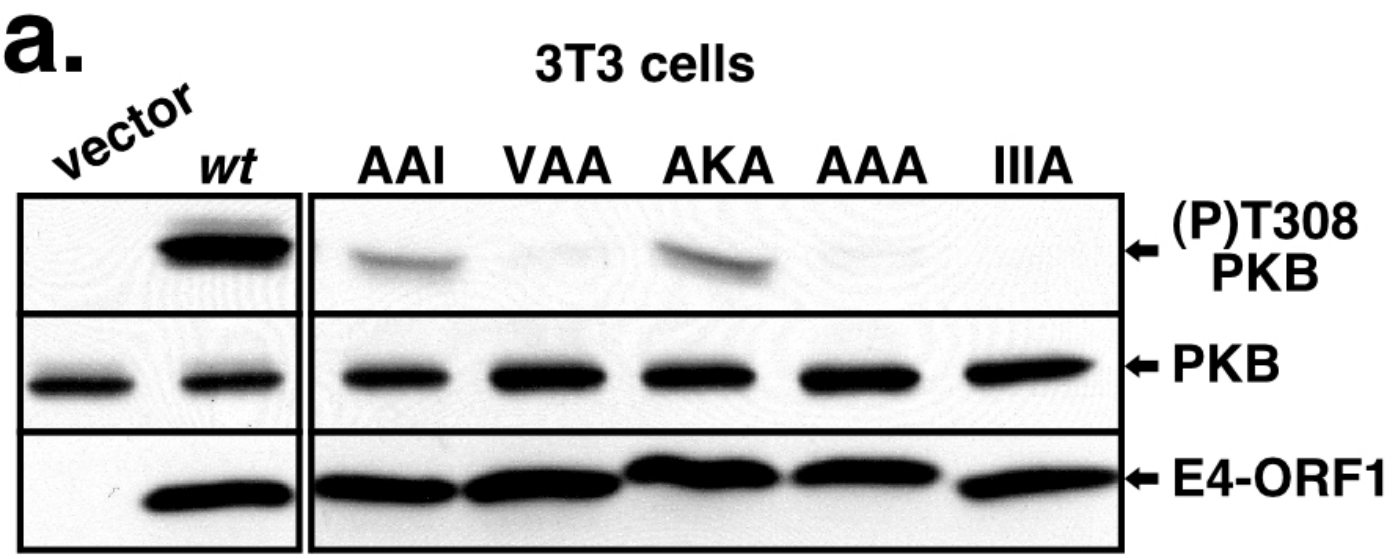
a.
3T3 cells
vector
wt
AAI
VAA
AKA
AAA
IIIA
(P)T308 PKB
PKB
E4-ORF1

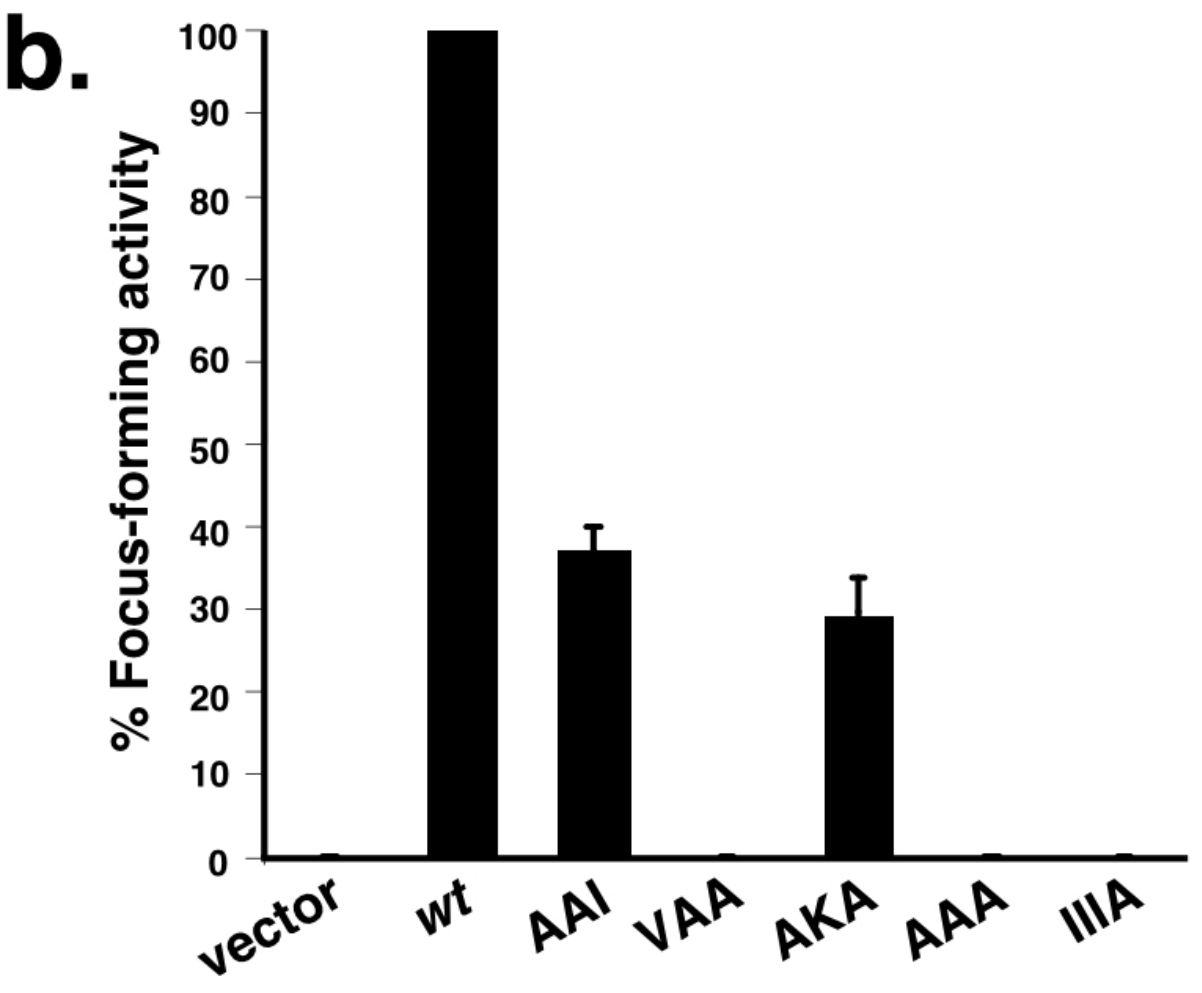
b.
% Focus-forming activity
100
90
80
70
60
50
40
30
20
10
0
vector
wt
AAI
VAA
AKA
AAA
IIIA

Fig. S10

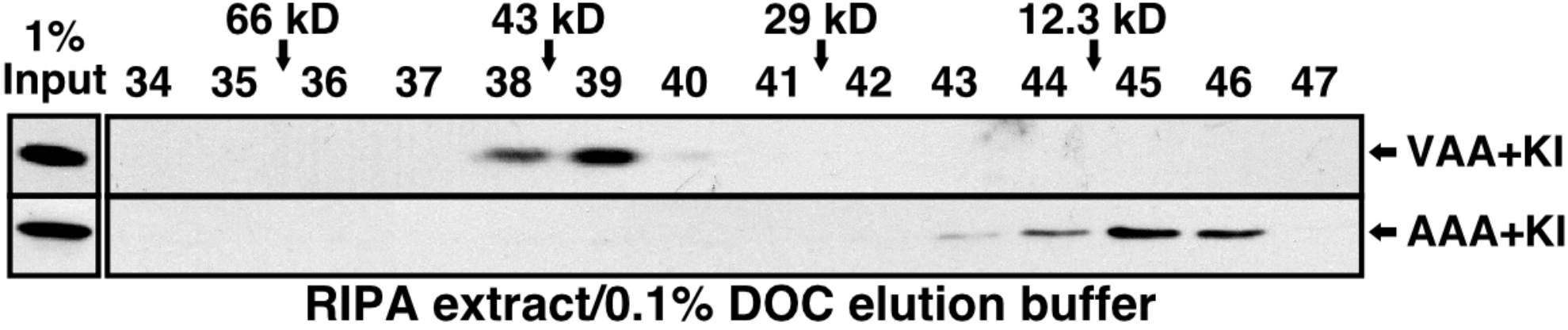
66 kD
43 kD
29 kD
12.3 kD
1% Input
34
35
36
37
38
39
40
41
42
43
44
45
46
47
VAA+KI
AAA+KI
RIPA extract/0.1% DOC elution buffer

Fig. S11

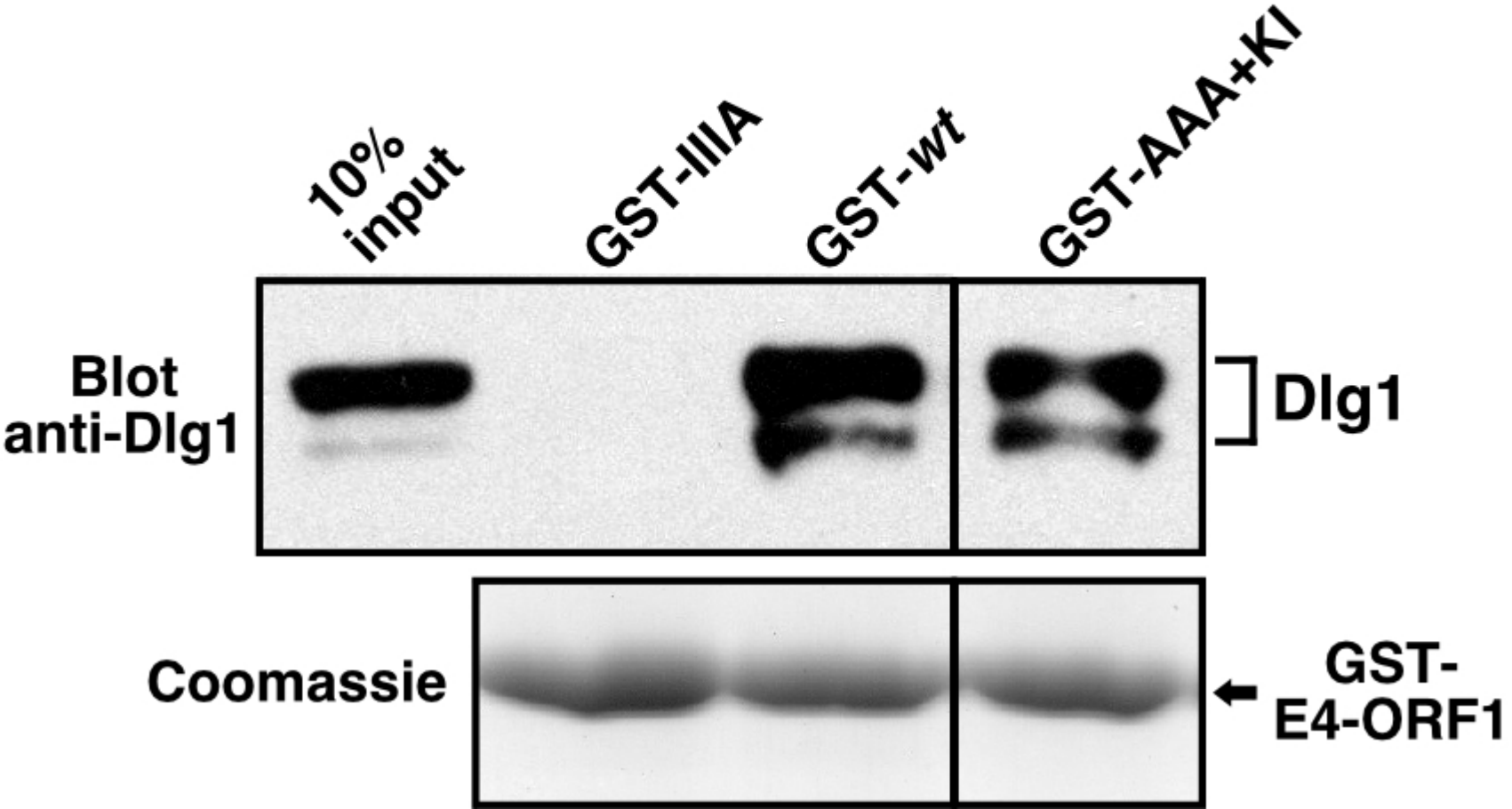
10% input
GST-IIIA
GST-wt
GST-AAA+KI
Blot anti-Dlg1
Dlg1
Coomassie
GST-E4-ORF1

Fig. S12

a.

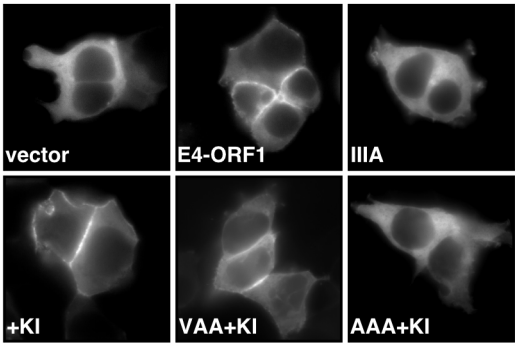
GFP-Dlg1 +
vector
E4-ORF1
IIIA
+KI
VAA+KI
AAA+KI

b.

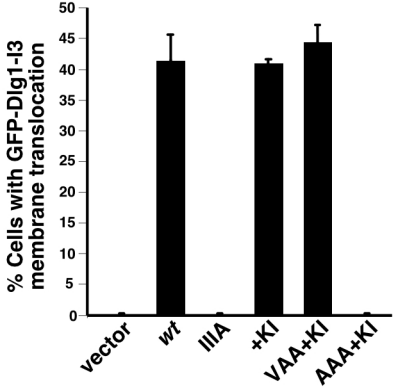
% Cells with GFP-Dlg1-I3 membrane translocation
50
45
40
35
30
25
20
15
10
5
0
vector
wt
IIIA
+KI
VAA+KI
AAA+KI

Fig. S13

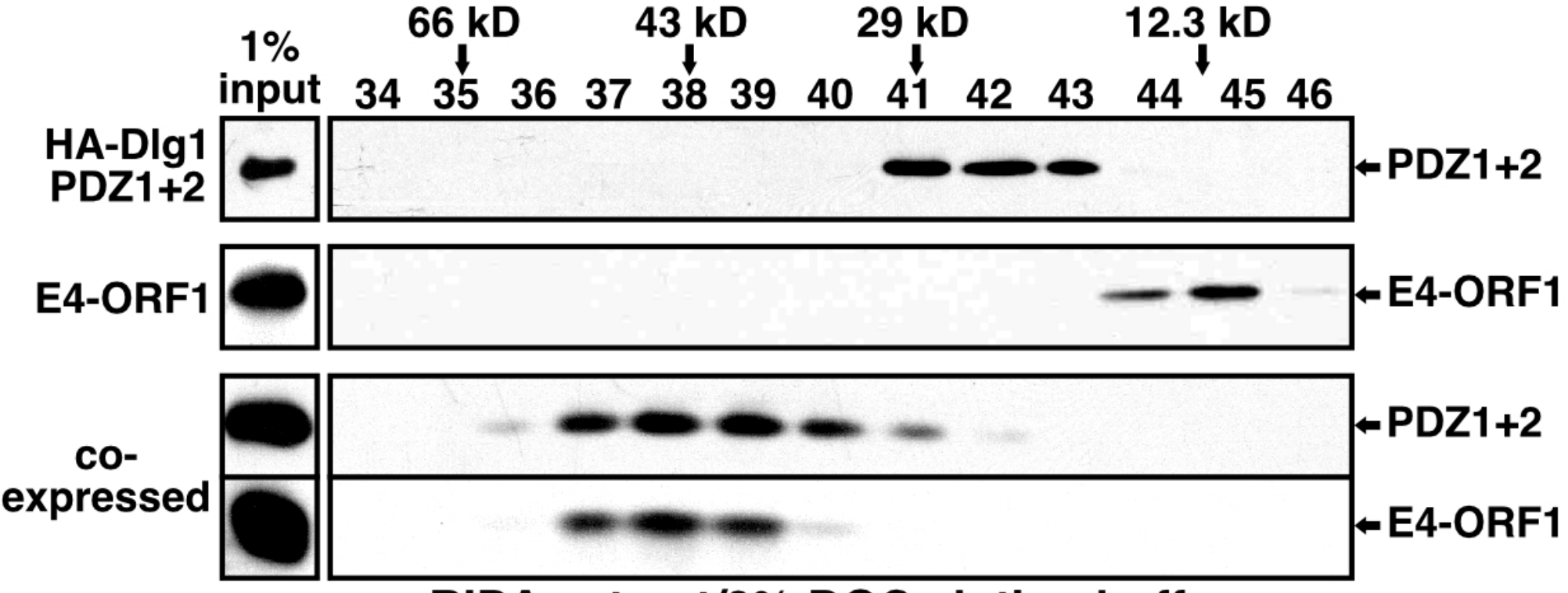
66 kD
43 kD
29 kD
12.3 kD
1% input
34 35 36 37 38 39 40 41 42 43 44 45 46
HA-Dlg1 PDZ1+2
E4-ORF1
co-expressed
PDZ1+2
E4-ORF1
PDZ1+2
E4-ORF1
RIPA extract/0% DOC elution buffer